

Cite this: *RSC Adv.*, 2017, **7**, 41713

## Individual and combined use of ginsenoside F2 and cyanidin-3-O-glucoside attenuates $H_2O_2$ -induced apoptosis in HEK-293 cells via the NF- $\kappa$ B pathway

Di Liu,<sup>a</sup> Ying Wang,<sup>b</sup> Shuang Ma,<sup>b</sup> Hongyu Sun,<sup>a</sup> Wenyan Shi<sup>a</sup> and Xianmin Feng  <sup>a</sup>

Ginsenosides have been regarded as the major active components of ginseng. Cyanidin-3-O-glucoside (C3G) is one of the best-known and investigated anthocyanins. Individual and combined protective effects of ginsenoside F2 and C3G against  $H_2O_2$ -induced apoptosis and the underlying mechanisms were explored in HEK-293 cells. The protein expression of cleaved caspase-3, Bcl-2, Bax, and cleaved PARP, and the levels of caspases-6, caspases-9, and lactate dehydrogenase (LDH), and mitochondria membrane potential (MMP) were measured as the apoptosis associated markers. The phosphorylation of nuclear factor kappa B (NF- $\kappa$ B) p65 was assessed by western blotting and qRT-PCR. When HEK-293 cells were stimulated with  $H_2O_2$ , individual F2 and C3G pre-incubation increased MMP, suppressed the leakage of LDH, significantly decreased the activities of caspases-6 and caspases-9, down-regulated the protein expression of cleaved caspase-3, Bax, and cleaved PARP, up-regulated the expression of Bcl-2, and down-regulated the protein and mRNA expressions of NF- $\kappa$ B p65. The synergistic effects were present in the combination F2 and C3G. The underlying mechanism of F2 and C3G in anti-apoptosis was in part relevant to the regulation of the mitochondria-mediated cell apoptotic pathway and the NF- $\kappa$ B pathway. The co-administration of F2 and C3G exhibited possible synergistic effects on the inhibition of  $H_2O_2$ -induced apoptosis.

Received 26th April 2017

Accepted 7th August 2017

DOI: 10.1039/c7ra04689h

[rsc.li/rsc-advances](http://rsc.li/rsc-advances)

## 1. Introduction

Apoptosis is a highly regulated process of cell death that plays a critical role in many important physiological disorders and diseases, such as cancer, autoimmunity, sepsis, and neurodegenerative diseases.<sup>1</sup> The significant events in apoptosis are linked to mitochondrial dysfunction and activation of many intracellular signaling pathways. The loss of mitochondrial membrane potential (MMP) results in the release of cytochrome c (cyto c) from mitochondria to cytosol, and in subsequently activating the caspase-cascade system.<sup>2,3</sup> The activation of the NF- $\kappa$ B signaling pathway is highly relevant to regulation of apoptosis in some model systems and cell types.<sup>4</sup>

The pharmacological effects of *P. ginseng* can be mainly attributed to the dammaren-type triterpenoids saponins, which are generally known as ginsenosides.<sup>5-7</sup> Several studies have shown that the ginsenoside metabolites are more active than protopanaxadiol-type (PPD-type) and protopanaxatriol-type (PPT-type) ginsenosides *in vitro* and *in vivo*.<sup>8-11</sup> Ginsenoside F2 (F2, Fig. 1A) can be converted from many PPD-type ginsenosides such as Rb1, Rb2, Rc and Rd by human intestinal microorganisms after oral ingestion.<sup>12</sup> The bioactivities of

ginsenoside F2 have been focused on its anti-cancer activity and the hair anagen induction effect.<sup>13-16</sup> Ginsenoside Rb1 and Rd, the precursors of ginsenoside F2, have been demonstrated that they can exhibit a potent effect on preventing external stimuli induced apoptosis in cells.<sup>17-19</sup> However, there is a dearth of information on the inhibition of  $H_2O_2$ -induced apoptosis by ginsenoside F2. Anthocyanins are natural colorants and anti-oxidants of the flavonoids family. Cyanidin-3-O-glucoside (C3G, Fig. 1B) is one of the best-known and investigated anthocyanins, which represents the main anthocyanin in the edible parts of several plants and shows beneficial effects in various human pathologies.<sup>20</sup> Several *in vitro* studies suggested that C3G is able to protect human endothelial cells against the alterations induced by TNF- $\alpha$  and palmitic acid through blocking the activation of NF- $\kappa$ B pathway.<sup>21,22</sup> C3G and its major metabolite FA attenuated the photooxidation-induced apoptosis by suppressing NF- $\kappa$ B activation *in vivo*.<sup>23</sup> Another study indicated that C3G is potentially able to counter  $H_2O_2$ -induced apoptosis efficiently by regulating the intrinsic apoptotic pathway associated proteins.<sup>24</sup>

In some cases the existence of synergic or antagonistic effects between the various components presents in a lot of plant food and derived products. Ginsenoside Rb1, one precursor of ginsenoside F2, has been demonstrated to exhibit synergistic effects with tanshinone IIA or salvianolic acid B on myocardial ischemia rats.<sup>25</sup> Some studies have demonstrated

<sup>a</sup>Department of Pathogenic Biology, Jilin Medical University, Jilin 132013, China.  
E-mail: [fengxianmin28@163.com](mailto:fengxianmin28@163.com)

<sup>b</sup>College of Food Science and Engineering, Jilin University, Changchun 130062, China



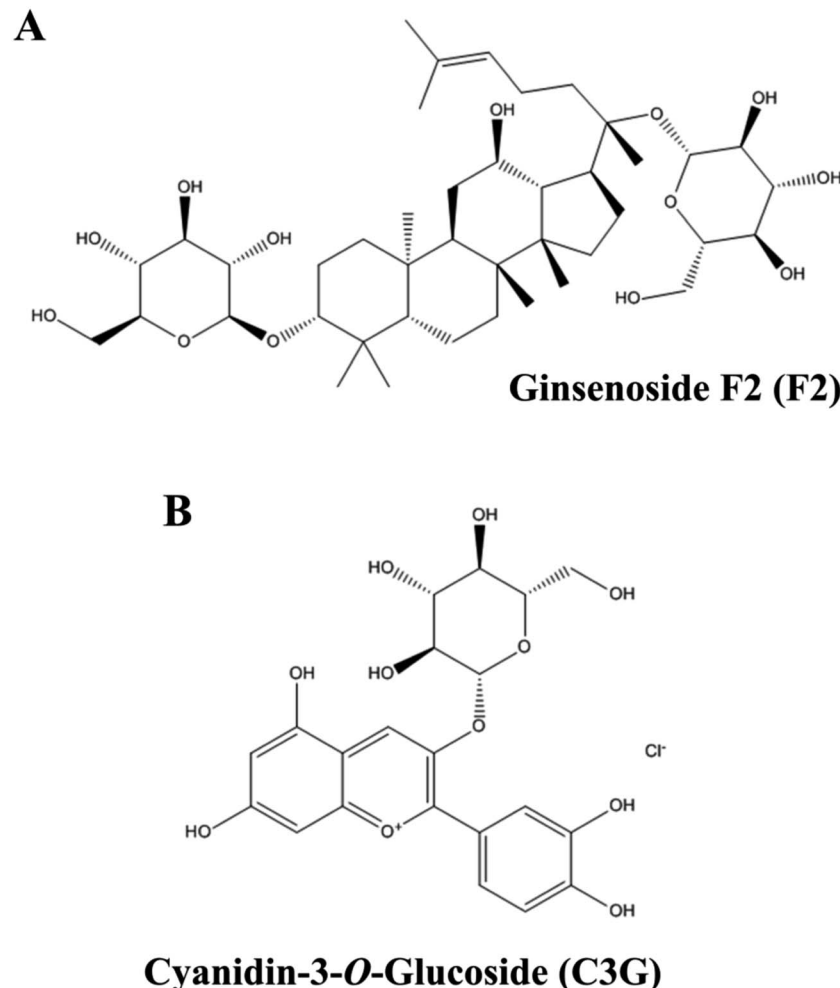


Fig. 1 Chemical structures of ginsenoside F2 (A) and cyanidin-3-O-glucoside (B).

that the dietary flavonoids, such as quercetin-3-*b*-glucoside, epicatechin, kaempferol and myricetin show synergistic effects with alpha-tocopherol or some other flavonoids.<sup>26,27</sup> Our previous study have demonstrated that F2 and C3G can protect HEK-293 cells against H<sub>2</sub>O<sub>2</sub>-induced oxidative stress and act synergy through reducing intracellular ROS and activating Nrf2/Keap1 signaling pathway.<sup>28</sup> However, until now very few studies have focused on the assessment of anthocyanins–ginsenosides interactions in terms of anti-apoptosis activity.

The HEK-293 cell line is an immortalized cell with normal renal-specific properties, which has been demonstrated to display several features of renal distal tubular cells with the epithelial morphology of apical zonulae occludentes and less pronounced brush-border.<sup>29,30</sup> Its metabolic conditions are more related to normal human cells compared with tumor cell.<sup>31</sup> It has been demonstrated to maintain important renal-specific properties and been used as cellular models of apoptosis, these was belong to its epithelial morphology.<sup>29,32,33</sup> Hydrogen peroxide (H<sub>2</sub>O<sub>2</sub>) has been extensively used to induce apoptosis *in vitro* models. Previous studies have demonstrated that H<sub>2</sub>O<sub>2</sub> induces apoptosis in cells *via* activating mitochondria-mediated apoptosis pathways<sup>32</sup> and NF-κB pathway.<sup>34</sup>

The aim of this study is to investigate the protective effects of ginsenoside F2 and C3G against H<sub>2</sub>O<sub>2</sub>-induced apoptosis in HEK-293 cells, and to determine whether the combination of F2 and C3G exerts synergistic effect on inhibiting apoptosis by regulating intrinsic apoptotic pathway-related proteins, NF-κB p65, cleaved caspase-3, Bcl-2, Bax, cleaved PARP, caspases 6 and caspases 9.

## 2. Materials and methods

### 2.1. Materials and chemicals

Ginsenoside F2 and cyanidin-3-O-glucoside (C3G) were purchased from the Chinese National Institute for the Control of Pharmaceutical and Biological Products, purity  $\geq 98\%$  (Beijing, China). DMEM, MEM Nonessential Amino Acids (MEM NEAA), Penicillin–Streptomycin Solution (PSS) and Fetal Bovine Serum (FBS) were obtained from Gibco (USA). The GoTaq Green Master Mix and Cell Titer 96® AQueous One Solution Cell Proliferation Assay (MTS) were purchased from Promega Biotechnology Co. Ltd. (Beijing, China). Lactate dehydrogenase (LDH), caspase-6 and caspase-9 assay kits were purchased from Nanjing Jiancheng Bioengineering CO. LTD (Nanjing, China,



www.njjcbio.com). Rainbow protein standard marker and D2000 DNA marker were purchased from Tiangen Biotech CO. LTD. (Beijing, China, www.tiangen.com). BCA protein assay kit, Enhanced Chemiluminescence (ECL) detection kit and Mitochondria Membrane Potential (MMP) assay kit were purchased from Beyotime Institute of Biotechnology (www.beyotime.com). RNase-free Water, PrimeScript™ RT Reagent Kit assay and SYBR fluorescent Premix were purchased from Takara Bioengineering Co. Ltd. Regular Agarose G-10 was obtained from Biowest. The antibodies against NF-κB p65 and GAPDH, goat anti-mouse and goat anti-rabbit antibodies were purchased from Wuhan Boster Biological Engineering Co., Ltd. (www.boster.com.cn). The antibodies against cleaved caspase-3, Bcl-2, Bax and cleaved poly (ADP-ribose) polymerase (cleaved PARP) were purchased from Cell Signaling Technology (Boston, MA, USA). Polyvinylidene fluoride (PVDF, 0.2  $\mu$ m) was purchased from Pall Corporation (America). Other chemicals were analytical grade.

## 2.2. Cell culture and treatment

The human embryonic kidney cell line (HEK-293 cells) was obtained from the Cell Bank of Type Culture Collection of the Chinese Academy of Sciences (Shanghai, China). HEK-293 cells were maintained in DMEM supplemented with 1% PSS, 10% FBS and 1% MEM NEAA in 5% CO<sub>2</sub> at 37 °C. Cells were seeded in flat-bottom 6-well or 12-well plates and incubated in a CO<sub>2</sub> incubator for 24 h, until all cells grown to 70–80% confluence. The cells were pretreated with ginsenoside F2, C3G and their combination (1.25, 5 and 20  $\mu$ M, volume proportion is 1 : 1) for 12 h and then were exposed to 400  $\mu$ M of H<sub>2</sub>O<sub>2</sub> for an additional 6 h in a humidified atmosphere of 5% CO<sub>2</sub>.

## 2.3. Assessments of ginsenoside F2 and C3G with variously combined ratio on cell viability

Normal HEK-293 cells without pretreatment were used as a control. The cells with treatment of H<sub>2</sub>O<sub>2</sub> were as an injury group. Cells were treated with the indicated concentrations (20  $\mu$ M) of F2, C3G and their combination with various ratios (1 : 1, 1 : 2, 2 : 1, 1 : 3, 3 : 1, 1 : 4, 4 : 1, 1 : 5, 5 : 1) for 12 h and H<sub>2</sub>O<sub>2</sub> (400  $\mu$ M) for 6 h. Cell viability was assessed by MTS assay. MTS (20  $\mu$ L) was added to the cultured cells incubated at 37 °C, 5% CO<sub>2</sub> for 1 hour. Then the plates were read in a multi-mode microplate reader (Bio Tek Instruments, USA) at 490 nm wavelength. The results were expressed as a percentage of corresponding values for the control group. All the experiments were repeated at least 3 times.

## 2.4. Cytotoxic and proliferation assessments of ginsenoside F2, C3G and their mixture

The ginsenoside F2 was dissolved in DMSO and DMEM medium, and C3G was dissolved in DMEM medium at different concentrations (1.25, 5 and 20  $\mu$ M). The mixture was made by mixing the ginsenoside F2 and the C3G with the volume proportion of 1 : 1, and the final concentrations were 1.25, 5 and 20  $\mu$ M. HEK-263 cells were seeded in a 96-well plate of 5 × 10<sup>3</sup> cells per well and incubated for 24 h. Then, the cells were

treated with ginsenoside F2, C3G and their mixture and were incubated for an additional 12 h at 37 °C, 5% CO<sub>2</sub>. Cell viability was determined using MTS method as described above.

## 2.5. Measurement of LDH release

The cells were washed once with PBS, then were lysed in ice-cold radio immunoprecipitation assay (RIPA) lysis buffer containing 1 mM phenylmethanesulfonyl fluoride (PMSF) for 10 min and centrifuged at 12 000g, 4 °C for 10 min. The LDH activities of medium and cell lysates were measured as the rate of consumption of NADH in the presence of pyruvate. A water-soluble tetrazolium salt (WST-1) was revert to colored formazan, which absorbance is at 450 nm. Then the absorbance was read in a multi-mode microplate reader (Bio Tek Instruments, USA) at 450 nm wavelength. The leakage of intracellular LDH into the medium was used to evaluate the cell damage, which corresponds to the ratio between the LDH activity in the medium and the total LDH activity.<sup>22</sup> LDH leakage rate was calculated as following equation:

$$\text{LDH release (\%)} = \frac{\text{LDH in the medium}}{\text{LDH in the medium} + \text{LDH in the cell}} \times 100.$$

## 2.6. Measurement of the mitochondrial membrane potential (MMP)

JC-1 fluorescent membrane dye has been used to analyze MMP in cells. A higher red/green ratio indicates a more polarized, or more negative and hyperpolarized, mitochondrial inner membrane.<sup>35</sup> Briefly, after the medium was removed, the cells were stained with JC-1 (5  $\mu$ M) for 20 min at 37 °C in 5% CO<sub>2</sub>, then washed with PBS for twice and added fresh medium. The green and red fluorescence images of JC-1 in HEK-293 cells were collected by Laser Scanning Confocal Microscopy (LSCM) (Olympus, Japan). The JC-1 fluorescence intensity was determined by a multi-mode microplate reader (Ex/Em of red: 525/590, Ex/Em of green: 490/530) and representation by ratio of red fluorescence/green fluorescence.

## 2.7. Measurement of caspase-6 and caspase-9 activities

Generally, the cells were washed once with PBS, then were lysed in ice-cold RIPA lysis buffer containing 1 mM PMSF for 15 min and centrifuged at 12 000g, 4 °C for 10 min. Activities of caspase-6 and caspase-9 levels were measured according to the spectrophotometric assay kit's protocols. The caspase-6/caspase-9 sequence-specific peptide is coupled to the chromophore group, and the chromophore group will free into the when the caspase-6/caspase-9 substrate is sheared. Then the activities of caspase-6/caspase-9 can be investigated by determining the absorbance of chromophore group at 405 nm or 400 nm. The absorbance was read in a multi-mode microplate reader at 405 nm wavelength. One enzymatic activity unit of caspase-6 (caspase-9) is the amount of enzyme that will cleave 1.0 nM of the colorimetric substrate Ac-VEID-PNA (Ac-LEHD-PNA) per hour at 37 °C under saturated substrate



concentrations. The units of enzymatic activity were calculated by standard curves of PNA.

### 2.8. Western blot analysis

Cultured cells were lysed in RIPA lysis buffer on ice for 10 min and centrifuged at 12 000g for 10 min. The total protein concentration was analyzed by BCA protein assay kit and 30 µg of the proteins were separated by 12% sodium dodecyl sulphate-polyacrylamide (SDS-PAGE) gels electrophoresis and were transferred onto PVDF membranes. The membranes were blocked with buffer (5% skim milk in Tris-buffered saline with 0.05% (v/v) Tween 20, TBST) at room temperature for 1 h and then incubated with antibodies against NF- $\kappa$ B p65 (1 : 400), cleaved caspase-3 (1 : 1000), Bcl-2 (1 : 1000), Bax (1 : 1000), cleaved PARP (1 : 1000) and GAPDH (1 : 1000) in TBST overnight at 4 °C. The membranes were washed three times with TBST and incubated with secondary antibodies (1 : 4000) for 1 h at room temperature. The protein bands on membranes were detected by DNR MiniBIS Pro Bio Imaging System (DNR, Israel) using ECL reagents. The collected images were quantitated by densitometric analysis using the ImageJ software (<http://rsb.info.nih.gov/ij/index.html>). The data of NF- $\kappa$ B p65, cleaved caspase-3, Bcl-2, Bax and cleaved PARP were normalized on the basis of GAPDH level.

### 2.9. Quantitative real-time polymerase chain reaction (qRT-PCR) analysis

For the quantification of gene expression, qRT-PCR was conducted by using SYBR Green on a real-time system (CFX96; Bio-Rad). Briefly, the total RNA of cells was extracted with TRIzol reagent and was detected by BioTek Epoch microplate spectrophotometer (BioTek, USA). The cDNA was reversely transcribed from total RNA after erasing gDNA by using a reverse transcriptase kit as described by the manufacturer. The qRT-PCR reaction contained 1 µg of cDNA, primers, RNase-free water and SYBR premix. Performed conditions were set as follow: 95 °C for 3 min, followed by 40 cycles of 95 °C for 15 s, 59 °C for 20 s and 72 °C for 30 s. The relative index of expression level was analyzed by  $2^{-\Delta\Delta Ct}$ . Expression level of NF- $\kappa$ B p65 gene was normalized by GAPDH level. All experiments were repeated at least three times. The sequences of the primer pairs used for the amplification of NF- $\kappa$ B p65 and GAPDH are as followed:

NF- $\kappa$ B p65 (forward primer: 5'-GGCGAATGGCTCGTCTG-3'; reverse primer: 5'-TTGGTGGTATCTGTGCTCCTCT-3'), GAPDH (forward primer: 5'-ATCCCACCACTCTCC-3'; reverse primer: 5'-CCATCACGCCACAGTTT-3').

### 2.10. Statistical analysis

All of the assays were carried out in triplicate. Data analyses were performed using the SPSS 21.0 software. The data were expressed as mean  $\pm$  standard deviation in the text and figures. The statistical significance of differences between two groups was determined by the one-way ANOVA program with the LSD test unless specified. The value of  $P < 0.05$  was considered significant.

## 3. Results

### 3.1. The effects of ginsenoside F2 and C3G with variously combined ratio on cell viability

The combined effects of ginsenoside F2, C3G with different ratios were investigated in pre-experiment by MTS assay. Fig. 2 showed that the cell viabilities of pretreatment groups were significant higher than that of the injury group ( $P < 0.05$ ). The combination of ginsenoside F2 and C3G with ratio of 1 : 1, 1 : 2 and 1 : 3 (F2 : C3G) exhibit significant increase compared with individual groups on cell viabilities ( $P < 0.05$ ). Furthermore, the cell viability of combination, which contains equal amounts of F2 and C3G, was higher than the groups with ratio of 1 : 2 and 1 : 3. The results implied that the combination with equal volume proportion showed stronger synergism. Thus, the ratio of 1 : 1 was chosen in subsequent experiments.

### 3.2. Cytotoxic and proliferative effects of ginsenoside F2, C3G and their mixture on HEK-293 cells

The effects of ginsenoside F2, C3G and their mixture on the viability of HEK-293 cells were evaluated by MTS assay. The ginsenoside F2, C3G and their mixture did not show significant stimulation or inhibition effect on the cell viability at 1.25, 5 and 20 µM (Fig. 3). The results indicated that the combination with equal volume proportion did not have cytotoxicity or proliferative effects. Thus the cell proliferative effect did not contribute to the inhibition effect of F2 or C3G or their combination on apoptotic. This range of concentration was used in the subsequent experiments.

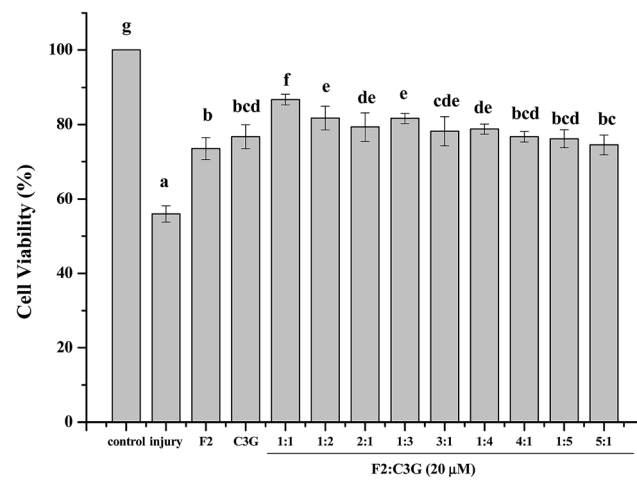


Fig. 2 The effects of ginsenoside F2 and C3G with variously combined ratio on cell viability. Cells were treated with the indicated concentrations (20 µM) of F2, C3G and their combination with various ratios for 12 h and H<sub>2</sub>O<sub>2</sub> (400 µM) for 6 h. Cell viability was assessed by MTS assay. The results were expressed as a percentage of corresponding values for the control group. Vertical bars indicate mean values  $\pm$  SD ( $n = 3$ ). Values with different letters indicate significant differences ( $P < 0.05$ ).



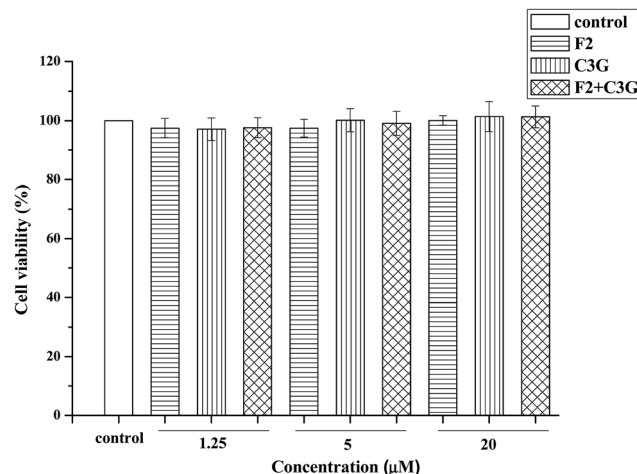


Fig. 3 Cytotoxic and proliferative effects of ginsenoside F2, C3G and their mixture in HEK-293 cells. Cells were treated with ginsenoside F2, C3G and their mixture at the indicated concentrations (1.25, 5 and 20  $\mu$ M) for 12 h. The mixture contains equal amounts of F2 and C3G. Cell viability was assessed by MTS assay. Vertical bars indicate mean values  $\pm$  SD ( $n = 3$ ).

### 3.3. Individual and combined effects of ginsenoside F2 and C3G on LDH release in HEK-293 cells

In this study, 400  $\mu$ M of  $H_2O_2$  and 6 h of incubating time were used to establish the  $H_2O_2$ -induced apoptosis model of HEK-293 cells according to our previous studies.<sup>31,32</sup> The leakage of LDH was used to evaluate the inhibitory effects of F2, C3G and their combination on  $H_2O_2$ -induced cytotoxicity. As shown in Fig. 4, the cells incubated with  $H_2O_2$  exhibited an increased

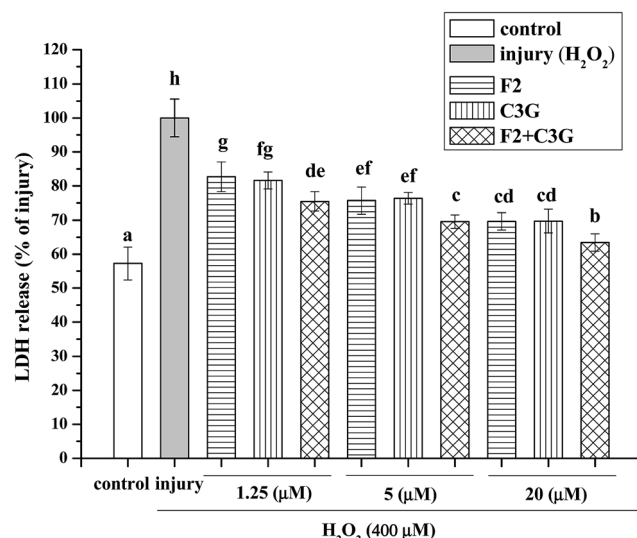


Fig. 4 Individual and combined effects of ginsenoside F2 and C3G on LDH release in HEK-293 cells. Cells were treated with the indicated concentrations (1.25, 5 and 20  $\mu$ M) of F2, C3G and their combination for 12 h and  $H_2O_2$  (400  $\mu$ M) for 6 h. LDH release was determined by LDH assay kit. The results were expressed as a percentage of corresponding values for the injury group. Vertical bars indicate mean values  $\pm$  SD ( $n = 3$ ). Values with different letters indicate significant differences ( $P < 0.05$ ).

level of LDH release compared with control group ( $P < 0.05$ ). However, F2 or C3G pretreatment resulted in a concentration-dependent reduction of the LDH release (Fig. 4). Moreover, when ginsenoside F2 was combined with C3G, significantly additional decreases of LDH release were observed at concentrations of 1.25, 5 and 20  $\mu$ M ( $p < 0.05$ , Fig. 4).

### 3.4. Individual and combined inhibiting effects of ginsenoside F2 and C3G on $H_2O_2$ -induced MMP loss in HEK-293 cells

To evaluate whether the ginsenoside F2 and C3G can inhibit MMP loss during the apoptosis induced by  $H_2O_2$ , HEK-293 cells were pretreated with ginsenoside F2, C3G and their combination at the indicated concentrations (1.25, 5 and 20  $\mu$ M) for 12 h and then were exposed to  $H_2O_2$  (400  $\mu$ M) for 6 h. Compared with the control group, MMP decreased considerably when cells were exposed to  $H_2O_2$  ( $P < 0.05$ , Fig. 5B). The green fluorescence increased and the red fluorescence decreased as shown in the confocal images (Fig. 5A). However, the intensity of red fluorescence increased along with the green decrease of green fluorescence in the F2 group and C3G group. Besides, the relative red/green ratios of the pretreatment groups were different from the  $H_2O_2$  group in a concentration-dependent manner ( $p < 0.05$ , Fig. 5). Compared with the single F2 or C3G pretreatment group, it was to see that stronger red fluorescence and weaker green fluorescence were shown in combination groups in Fig. 5A. And additional promoted effects on red/green ratios were observed at concentrations of 1.25, 5 and 20  $\mu$ M ( $p < 0.05$ , Fig. 5B).

### 3.5. Individual and combined effects of ginsenoside F2 and C3G on activities of caspase-6 and caspase-9 in HEK-293 cells

Caspase-6 and caspase-9 as the main proteins of caspase family can be activated by  $H_2O_2$  and act as the indices of apoptosis. To evaluate the effects of F2 and C3G on attenuation of apoptosis, the activities of caspase-6 and caspase-9 were measured in cultured HEK-293 cells. In Fig. 6, when HEK-293 cells were exposed to 400  $\mu$ M  $H_2O_2$ , the activities of caspase-6 and caspase-9 increased significantly compared with the control group ( $p < 0.05$ ). In contrast, both ginsenoside F2 and C3G pretreatment groups exhibited concentration-dependent suppression of caspase-6 and caspase-9 activities. With the intervention of the combination, the activities of caspase-6 and caspase-9 increased much more compared with a single F2 or C3G pretreatment at the corresponding concentration (1.25, 5 and 20  $\mu$ M,  $p < 0.05$ , Fig. 6).

### 3.6. Individual and combined effects of ginsenoside F2 and C3G on protein expression levels of cleaved caspase-3, Bcl-2, Bax and cleaved PARP

To further confirm the inhibitory effects of individual and combined use of F2 and C3G on  $H_2O_2$ -induced apoptosis, expression levels of apoptosis related proteins, such as cleaved caspase-3, Bcl-2, Bax and cleaved PARP, were analyzed by western blot analyses. As shown in Fig. 7, when cells were exposed to  $H_2O_2$ , an increase in the cleaved form of caspase-3



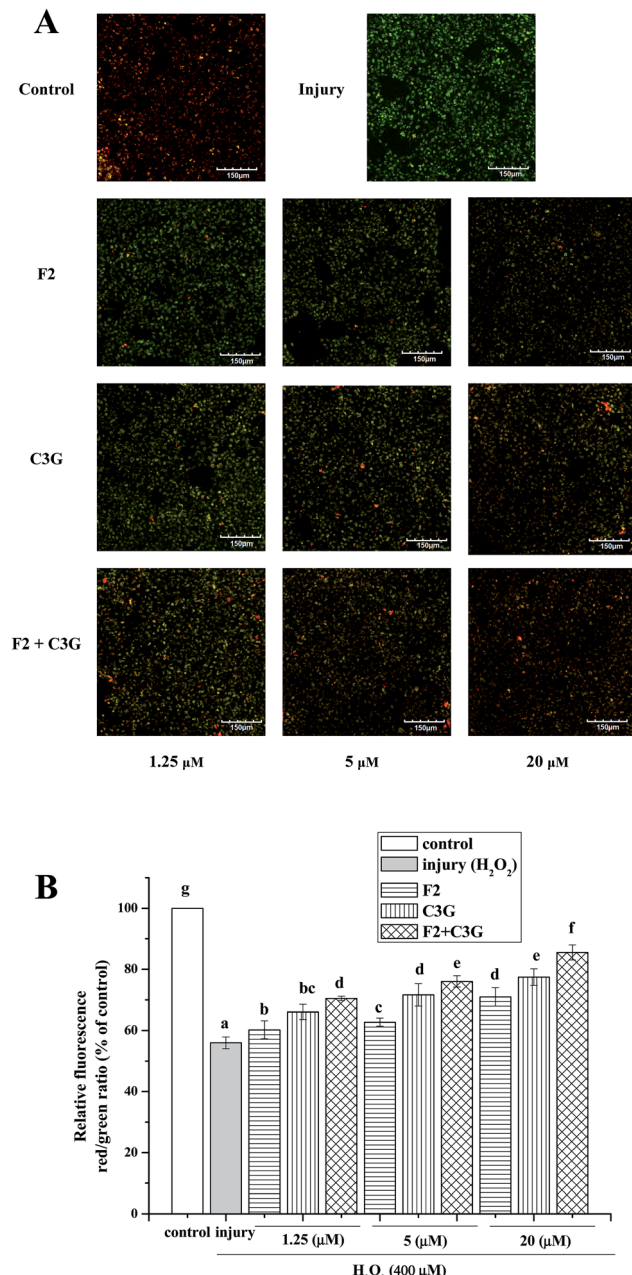


**Fig. 5** Individual and combined effects of ginsenoside F2 and C3G on inhibition of  $\text{H}_2\text{O}_2$ -induced MMP loss in HEK-293 cells. MMP was measured by fluorescence intensity after staining cells with JC-1. (A) Confocal images of fluorescence in HEK-293 cells. (B) MMP loss was represented by relative red/green ratio of fluorescence. The red/green ratio in the control group was designed as 1.0 and that was used to express the relative fluorescence intensity in other groups. Vertical bars indicate mean values  $\pm$  SD ( $n = 3$ ). Values with different letters indicate significant differences ( $P < 0.05$ ).

was observed compared with the control cells ( $P < 0.05$ , Fig. 7A), as well as a significant increase in cleaved PARP protein and reduction in Bcl-2/Bax ratio ( $P < 0.05$ , Fig. 7B and C). However, the pretreatment of C3G noticeably reversed the  $\text{H}_2\text{O}_2$ -induced cleaved caspase-3 generation, Bcl-2 down-regulation, Bax and PARP up-regulation in a concentration-dependent manner ( $P < 0.05$ , Fig. 7). The F2 pretreatment resulted in reductions of

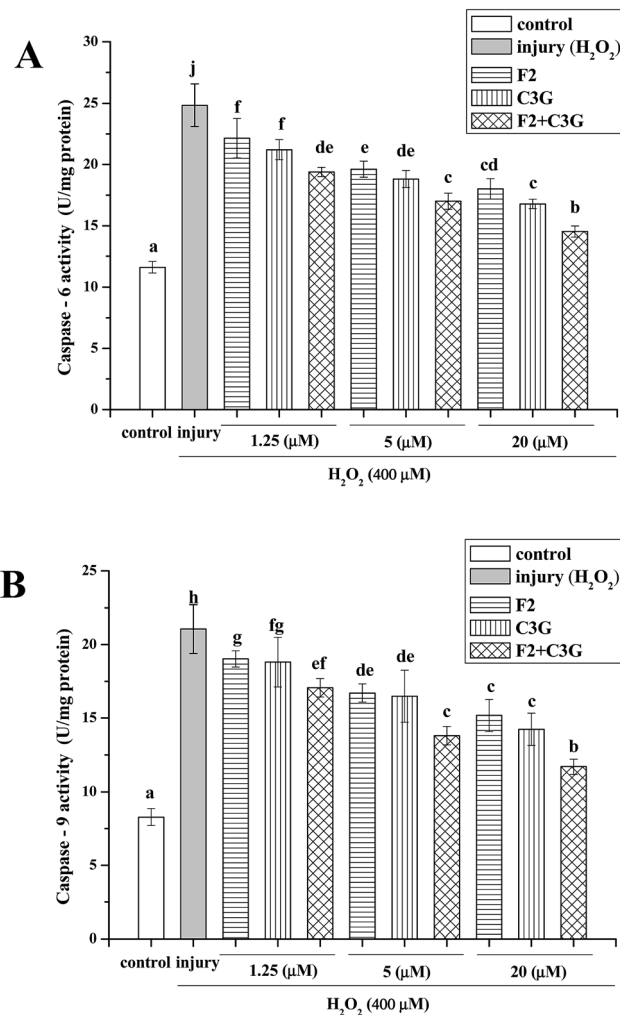


**Fig. 6** Individual and combined effects of ginsenoside F2 and C3G on activities of caspase-6 (A) and caspase-9 (B) in HEK-293 cells. Cells were treated with indicated concentrations (1.25, 5 and 20  $\mu\text{M}$ ) of F2, C3G and their combination for 12 h and  $\text{H}_2\text{O}_2$  (400  $\mu\text{M}$ ) for 6 h. Cellular caspase-6 (A) and caspase-9 (B) were measured with corresponding assay kits. Vertical bars indicate mean values  $\pm$  SD ( $n = 3$ ). Values with different letters indicate significant differences ( $P < 0.05$ ).

cleaved caspase-3 and cleaved PARP, and significant increases in Bcl-2/Bax ratio at concentrations of 5  $\mu\text{M}$  and 20  $\mu\text{M}$  ( $P < 0.05$ , Fig. 7). Additionally, when F2 was added together with C3G, pronouncedly additional decreases of cleaved caspase-3, cleaved PARP, and increases of Bcl-2/Bax ratio were observed compared with the single F2 or C3G group ( $p < 0.05$ , Fig. 7).

### 3.7. Individual and combined effects of ginsenoside F2 and C3G on protein and mRNA expression levels of NF- $\kappa$ B p65

To further explore the underlying mechanisms of ginsenoside F2 and C3G on  $\text{H}_2\text{O}_2$ -induced apoptosis *in vitro*, the transcription factor NF- $\kappa$ B was analyzed by western blot and qRT-PCR. As shown in Fig. 8, the injury group displayed a significant increase in protein expression of NF- $\kappa$ B p65, followed by an up-regulation of mRNA expression compared with the control group ( $P < 0.05$ ). In contrast, both ginsenoside F2 and C3G

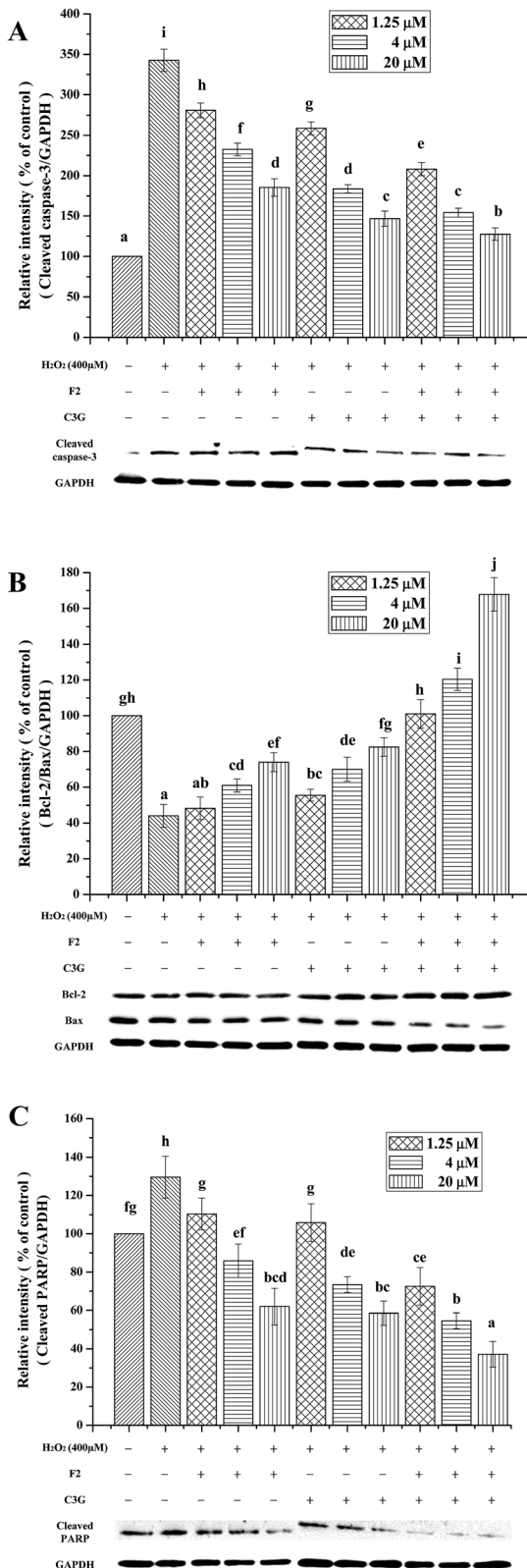


**Fig. 7** Individual and combined effects of ginsenoside F2 and C3G on the protein expression levels of cleaved caspase-3 (A), Bcl-2/Bax (B) and cleaved PARP (C). The protein expression levels were determined by western blot. The intensity of the band was quantitated by density analysis and expressed as a ratio of control group on the basis of GAPDH level (set to 100%). Vertical bars indicate mean values  $\pm$  SD ( $n = 3$ ). Values with different letters indicate significant differences ( $P < 0.05$ ).

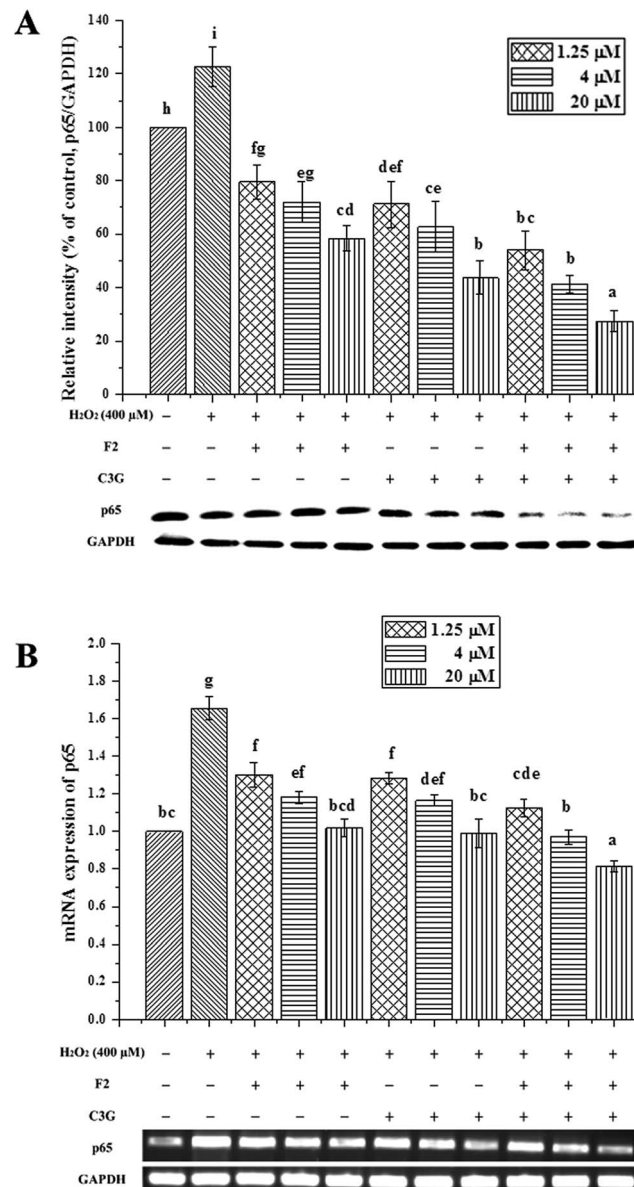


**Fig. 8** Individual and combined effects of ginsenoside F2 and C3G on protein and mRNA expression levels of NF- $\kappa$ B p65. The protein and mRNA expression levels of p65 and GAPDH were determined by western blot and qRT-PCR, respectively. The intensity of the protein band was quantitated by densitometric analysis and expressed as a ratio of control group (set to 100%). Vertical bars indicate mean values  $\pm$  SD ( $n = 3$ ). Values with different letters indicate significant differences ( $P < 0.05$ ).

pretreatment resulted in significant decreases in the protein expressions of p65 ( $P < 0.05$ , Fig. 8A). The mRNA expressions of p65 were noticeably down-regulated by individual F2 or C3G in a concentration-dependent manner ( $P < 0.05$ , Fig. 8B). In addition, we investigated the combined effects of F2 and C3G in apoptotic cells. The results showed that, when 0.625  $\mu$ M ginsenoside F2 was combined with 0.625  $\mu$ M C3G, the protein and mRNA expression levels of p65 were lower than those of individual treatment of 1.25  $\mu$ M F2 or 1.25  $\mu$ M C3G ( $p < 0.05$ ), as well in the concentrations of 5 and 20  $\mu$ M ( $p < 0.05$ , Fig. 8).

## 4. Discussion

Exogenous  $H_2O_2$  can traverse cell membranes, causing the generation and accumulation of ROS, uncoupling the electron transport chain in the mitochondria, leading a decrease in mitochondrial membrane potential and DNA damage.<sup>24,36</sup> It can also lead the cytosolic mobilization of Cyt c, activate the mitochondrial-mediated apoptosis pathway and, in consequence, induce cell apoptotic. In the present study, an  $H_2O_2$ -induced HEK-293 cell apoptosis model was used to investigate the anti-apoptosis effect of ginsenoside F2 and C3G. In this work, different ratios of combination were investigated in pre-experiment, and the combination with equal volume proportion showed stronger synergism. The cell viabilities of HEK-293 cells with pretreatments were not increased or decreased significantly at the concentrations from 1.25 to 20  $\mu M$ , which implied that the F2, C3G and their combination did not exert cytotoxic and proliferative effects on HEK-293 cells at the varying concentrations ranging from 1.25 to 20  $\mu M$  (Fig. 3). Thus, the inhibitory effects of F2, C3G and their combination against apoptosis were not due to the cell cytotoxicity effects.

The synergistic effects were analyzed by the direct comparison methodology which was reported by Kuei-long Liao.<sup>37</sup> The results showed that the individual and combined use of F2 and C3G inhibited apoptosis induced by  $H_2O_2$  in HEK-293 cells, by ameliorating LDH release and MMP loss, regulating the proteins associated with apoptosis, suppressing the phosphorylation of p65 and thus inhibiting the activation of NF- $\kappa B$  signaling pathway.

The status of cellular LDH leakage can be used to evaluate the  $H_2O_2$ -induced cytotoxicity and plasma membrane damage by measuring the activity of lactate dehydrogenase released from injured cells.<sup>38</sup> The decrease of MMP is regarded as one of the early events being associated with apoptosis, which occurs when cells are exposed to  $H_2O_2$ . The MMP loss leads to generation of ROS, release of apoptotic related proteins from mitochondria, and caspase-dependent apoptosis subsequently.<sup>39</sup> The results showed that F2 and C3G significantly reduced the LDH leakage and alleviated the MMP reduction in  $H_2O_2$ -stimulated HEK-293 cells, which implied that the anti-apoptotic effects of F2 and C3G might be related to the stabilization of LDH and MMP. Moreover, the combined pretreatment of ginsenoside F2 and C3G exhibited stronger inhibitions of the LDH leakage and MMP loss than the single pretreatment (Fig. 4 and 5). Previous studies have indicated that mitochondria-related apoptosis pathways are associated with  $H_2O_2$ -induced LDH release and MMP loss in SH-SY5Y cells.<sup>40</sup> Besides, if combination of 5  $\mu M$  substance A plus 5  $\mu M$  substance B shows greater effects than 10  $\mu M$  A (or B) treatment alone, it means there is a synergistic effect between A and B.<sup>37</sup> Thus, the results provided the evidence that F2 and C3G may synergistically mediate the  $H_2O_2$ -induced apoptosis, probably in part due to their improved abilities of preventing the plasma membrane damage and MMP loss.

The mitochondrial pathway is one of the distinct mechanisms in inducing cell apoptosis, which is influenced by the

rheostat of pro- and anti-apoptotic proteins of the Bcl-2 family and accompanied by exhibited of caspases.<sup>41,42</sup> The proteins of the Bcl-2 family are intimately associated with the regulation of MMP, and the subsequent release of cytochrome c from the mitochondrial intermembrane space.<sup>43</sup> As a key pro-apoptotic member of the Bcl-2 family, Bax can interact with pore proteins on the mitochondrial membrane and decrease the MMP, which results in initiation of the caspase pathway for apoptosis, such as activating caspase-9 and caspase-6. Caspase-9 is the most upstream member of the apoptotic protease cascade, which is directly activated by cytochrome c and Apaf-1. The activated caspase-9 in turn activates the most critical enzyme caspase-3 by cleaving caspase-3 at its N-terminal.<sup>33</sup> Cleaved caspase-3 and caspase-6 subsequently activate downstream substrate PARP, which will cleave and promote cellular disintegration, and eventually lead to cell apoptosis. In our study, we found that the activities of caspase-6 and caspase-9 in  $H_2O_2$ -treated cells increase considerably compared with the control cells. However, the pretreatment with F2 or C3G can reverse this situation in a dose-dependent manner (Fig. 6). In addition, we found that F2 and C3G could increase the ratio of Bcl-2/Bax compared with the  $H_2O_2$ -stimulated cells and decrease the protein expressions of cleaved caspase-3 and cleaved PARP (Fig. 7). These results demonstrated that the anti-apoptotic effects of both F2 and C3G were partly due to their mediation of  $H_2O_2$ -induced mitochondrial dysfunction. Parallel to our study, a study by Mai, T. T. *et al.* also revealed that F2 displays its anti-proliferative activity against breast cancer stem cells by regulating the mitochondrial membrane degradation and the levels of Bax, Bcl-2, PARP and cleaved caspase-9.<sup>14</sup> Rd, a precursor of ginsenoside F2, was found to protect neurons from apoptosis through increasing the expression of Bcl-2, decreasing the level of Bax, and suppressing the expression of cleaved caspase-3.<sup>19</sup> The previous study also demonstrated that C3G protects biological systems against the cytotoxic effects partly by reducing the peroxynitrite-induced activation of PARP in HUVECs.<sup>44</sup> The combination of heat shock protein 70 and ginsenoside Rg1 has been found to significantly block neurons apoptosis and reduce neural cytotoxicity in co-cultured cells, *via* affecting caspase-3 and remodeling of the synapsis.<sup>45</sup> These published data lead us to determine the synergistic effects of F2 and C3G and the underlying mechanisms. Our results showed that when the HEK-293 cells were co-administrated with F2 and C3G, the ratio of Bcl-2/Bax increased significantly compared with the individual group, the activities of caspase-6 and caspase-9 decreased more than either of the single pretreatment, as well as the protein levels of cleaved caspase-3 and cleaved PARP (Fig. 6 and 7). These results suggested that the combination exhibited a potentially synergistic effect on apoptosis resistance *via* inhibiting the mitochondria dependent apoptotic pathways.

NF- $\kappa B$  signaling pathway, which comprises a family of transcription factors, plays an important role in apoptosis and enables cells to adapt to intestinal environmental changes.<sup>46</sup> The phosphorylation of dimer subunits is important for the transcriptional activity of NF- $\kappa B$ , for example the phosphorylation of p65 has been shown to positively involve



in its transcriptional activity.<sup>47</sup> Previous study has suggested that NF- $\kappa$ B plays a pivotal role in maintaining renal function that also involved regulating RelA/p65 levels during folic acid induced acute kidney injury.<sup>48</sup> NF- $\kappa$ B and Nrf2 are important regulators of oxidation resistance and contribute to the pathogenesis of many diseases.<sup>49</sup> Several studies have demonstrated that C3G can protect human endothelial cells against dysfunction through activating the Nrf2 related pathway and blocking the activation of NF- $\kappa$ B pathway.<sup>21,22,50</sup> Our previous study has demonstrated that F2 and C3G can protect HEK-293 cells against H<sub>2</sub>O<sub>2</sub>-induced oxidative stress by activating Nrf2/Keap1 signaling pathway. In the current research, the H<sub>2</sub>O<sub>2</sub>-induced increase in protein and mRNA expressions of p65 was inhibited by ginsenoside F2 and C3G respectively in a dose-dependent manner (Fig. 8). These results suggested that F2 and C3G restrained H<sub>2</sub>O<sub>2</sub>-induced apoptosis *via* down-regulating the expression of p65 and inhibiting the activation of NF- $\kappa$ B pathway. Ginsenoside Rh3, one metabolite of PPD-type ginsenosides, was reported to inhibit NF- $\kappa$ B pathway by increasing the DNA-binding activity of Nrf2 in cultured cells.<sup>51</sup> The synergistic effect of ginsenoside Rg3 and docetaxel has been previously reported. Kim *et al.* reported that when Rg3 was combined with docetaxel the chemosensitivity would enhance in cisplatin-sensitive cells.<sup>52</sup> Compared with the individual pretreatment, the expression of p65 was decreased significantly when the cells were co-administrated with F2 and C3G (Fig. 8). These results suggested that the synergistically anti-apoptotic effect of F2 and C3G was mediated through NF- $\kappa$ B pathway. Combined with our previous study, the Nrf2/Keap1 and NF- $\kappa$ B pathways are reversed in oxidative stress induced apoptosis. Similar study has revealed that, the NF- $\kappa$ B p65 subunit negative regulate the Nrf2-ARE pathway by competing for recruitment of the transcription co-activator CBP and HDAC3.<sup>53</sup> Moreover, NF- $\kappa$ B signal pathway inhibits the Nrf2 signaling through interaction of p65 and Keap1.<sup>54</sup>

## 5. Conclusion

In summary, our results for the first time demonstrated that ginsenoside F2 and C3G could inhibit apoptosis induced by H<sub>2</sub>O<sub>2</sub> in HEK-293 cells. The potential underlying mechanisms were associated with several different aspects, including the amelioration of LDH release and MMP loss, the regulation of the proteins associated with apoptosis, the suppression of the phosphorylation of p65 thus inhibited the activation of NF- $\kappa$ B signaling pathway. Moreover, the co-administrations of F2 and C3G exhibited synergistic effects on inhibition of H<sub>2</sub>O<sub>2</sub>-induced apoptosis, which was related to the regulation of mitochondria-mediated cell apoptotic pathway and NF- $\kappa$ B pathway. These findings revealed that, the combination use of F2 and C3G seems to be a beneficial method in mitigation of a variety of apoptosis-induced disorders. However, further studies are also needed to investigate other potential aspects of synergistic effects, such as anti-inflammation, and to testify the underlying mechanisms *in vivo*.

## Conflicts of interest

The authors have declared no conflict of interest.

## Abbreviations

|                               |  |
|-------------------------------|--|
| Bcl-2                         | B-cell lymphoma-2  |
| Bax                           | Bcl 2-associated X protein                                       |
| C3G                           | Cyanidin-3-O-glucoside   |
| F2                            | Ginsenoside F2   |
| HEK-293                       | Human embryonic kidney cell                                      |
| H <sub>2</sub> O <sub>2</sub> | Hydrogen peroxide  |
| LDH                           | Lactate dehydrogenase  |
| MMP                           | Mitochondrial membrane potential                                 |
| NF- $\kappa$ B                | Nuclear factor 'kappa-light-chain-enhancer' of activated B-cells |
| PARP                          | Poly ADP-ribose polymerase                                       |

## Acknowledgements

This work was partially supported by the National Natural Science Foundation of China (No. 31471597 and No. 31572262). And Chinese medicine science and technology project of Jilin province (No. 2017104).

## References

- 1 P. C. A. Kam and N. I. Ferch, *Anaesthesia*, 2000, **55**, 1081–1093.
- 2 N. A. Thornberry and Y. Lazebnik, *Science*, 1998, **281**, 1312–1316.
- 3 D. R. Green and J. C. Reed, *Science*, 1998, **281**, 1309–1312.
- 4 J. L. Martindale and N. J. Holbrook, *J. Cell. Physiol.*, 2002, **192**, 1–15.
- 5 Y.-E. An, S.-C. Ahn, D.-C. Yang, S.-J. Park, B.-Y. Kim and M.-Y. Baik, *LWT-Food Sci. Technol.*, 2011, **44**, 370–374.
- 6 A. S. Attele, J. A. Wu and C. S. Yuan, *Biochem. Pharmacol.*, 1999, **58**, 1685–1693.
- 7 D. O. Kennedy and A. B. Scholey, *Pharmacol., Biochem. Behav.*, 2003, **75**, 687–700.
- 8 B. G. Kim, S. Y. Choi, M. R. Kim, H. J. Suh and H. J. Park, *Process Biochem.*, 2010, **45**, 1319–1324.
- 9 L. W. Qi, C. Z. Wang and C. S. Yuan, *Biochem. Pharmacol.*, 2010, **80**, 947–954.
- 10 Z. Q. Liu, X. Y. Luo, G. Z. Liu, Y. P. Chen, Z. C. Wang and Y. X. Sun, *J. Agric. Food Chem.*, 2003, **51**, 2555–2558.
- 11 M. A. Tawab, U. Bahr, M. Karas, M. Wurglics and M. Schubert-Zsilavecz, *Drug Metab. Dispos.*, 2003, **31**, 1065–1071.
- 12 S. Ko, Y. Suzuki, K. Suzuki, K. Choi and B. Cho, *Chem. Pharm. Bull.*, 2007, **55**, 1522–1527.
- 13 J. Y. Shin, J. M. Lee, H. S. Shin, S. Y. Park, J. E. Yang, S. K. Cho and T. H. Yi, *J. Ginseng Res.*, 2012, **36**, 86–92.
- 14 T. T. Mai, J. Moon, Y. Song, P. Q. Viet, P. V. Phuc, J. M. Lee, T. H. Yi, M. Cho and S. K. Cho, *Cancer Lett.*, 2012, **321**, 144–153.



15 H. S. Shin, S. Y. Park, E. S. Hwang, D. G. Lee, G. T. Mavlonov and T. H. Yi, *Biol. Pharm. Bull.*, 2014, **37**, 755–763.

16 H. S. Shin, S. Y. Park, E. S. Hwang, D. G. Lee, H. G. Song, G. T. Mavlonov and T. H. Yi, *Eur. J. Pharmacol.*, 2014, **730**, 82–89.

17 B. X. Cai, S. L. Jin, D. Luo, X. F. Lin and J. Gao, *Biol. Pharm. Bull.*, 2009, **32**, 837–841.

18 B. Xue, L. Q. Sun, X. J. Li, X. Wang, Y. Zhang, Y. M. Mu and L. L. Liang, *Neural Regener. Res.*, 2012, **7**, 2340–2346.

19 J. F. Liu, X. D. Yan, L. S. Qi, L. Li, G. Y. Hu, P. Li and G. Zhao, *Chem.-Biol. Interact.*, 2015, **239**, 12–18.

20 J. Kong, *Phytochemistry*, 2003, **64**, 923–933.

21 D. Fratantonio, A. Speciale, D. Ferrari, M. Cristani, A. Saija and F. Cimino, *Toxicol. Lett.*, 2015, **239**, 152–160.

22 A. Speciale, R. Canali, J. Chirafisi, A. Saija, F. Virgili and F. Cimino, *J. Agric. Food Chem.*, 2010, **58**, 12048–12054.

23 Y. Wang, Y. Huo, L. Zhao, F. Lu, O. Wang, X. Yang, B. Ji and F. Zhou, *Mol. Nutr. Food Res.*, 2016, **60**, 1564–1577.

24 J. S. Lee, Y. R. Kim, I. G. Song, S. J. Ha, Y. E. Kim, N. I. Baek and E. K. Hong, *Int. J. Mol. Med.*, 2015, **35**, 405–412.

25 Y. Lu, X. Liu, X. Liang, L. Xiang and W. Zhang, *J. Ethnopharmacol.*, 2011, **134**, 45–49.

26 J. Frank, A. Budek, T. Lundh, R. S. Parker, J. E. Swanson, C. F. Lourenco, B. Gago, J. Laranjinha, B. Vessby and A. Kamal-Eldin, *J. Lipid Res.*, 2006, **47**, 2718–2725.

27 M. Hidalgo, C. Sánchez-Moreno and S. de Pascual-Teresa, *Food Chem.*, 2010, **121**, 691–696.

28 D. Liu, F. Pan, J. Liu, Y. Wang, T. Zhang, E. Wang and J. Liu, *RSC Adv.*, 2016, **6**, 81092–81100.

29 N. L. Simmons, *Exp. Physiol.*, 1990, **75**, 309–319.

30 A. I. Serban, L. Stanca, O. I. Geicu and A. Dinischiotu, *Int. J. Mol. Sci.*, 2015, **16**, 20100–20117.

31 D. Liu, T. Zhang, Z. Chen, Y. Wang, S. Ma, J. Liu and J. Liu, *J. Ginseng Res.*, 2016, **41**, 169–179.

32 J. B. Liu, Z. F. Chen, J. He, Y. Zhang, T. Zhang and Y. Q. Jiang, *Food Funct.*, 2014, **5**, 3179–3188.

33 P. Li, D. Nijhawan, I. Budihardjo, S. M. Srinivasula, M. Ahmad, E. S. Alnemri and X. Wang, *Cell*, 1997, **91**, 479–489.

34 X. Zeng, X. Zhou, L. Cui, D. Liu, K. Wu, W. Li and R. Huang, *Molecules*, 2014, **19**, 7368–7387.

35 L. Sun, J. Zhang, K. Fang, Y. Ding, L. Zhang and Y. Zhang, *Food Funct.*, 2014, **5**, 471–479.

36 M. V. Naval, M. P. Gomez-Serranillos, M. E. Carretero and A. M. Villar, *J. Ethnopharmacol.*, 2007, **112**, 262–270.

37 K. L. Liao and M. C. Yin, *J. Agric. Food Chem.*, 2000, **48**, 2266–2270.

38 Y. R. Zhao, W. Qu, W. Y. Liu, H. Hong, F. Feng, H. Chen and N. Xie, *Chin. J. Nat. Med.*, 2015, **13**, 438–444.

39 J. Lago, F. Santaclara, J. M. Vieites and A. G. Cabado, *Toxicon*, 2005, **46**, 579–586.

40 X. L. Hu, Y. X. Niu, Q. Zhang, X. Tian, L. Y. Gao, L. P. Guo, W. H. Meng and Q. C. Zhao, *Environ. Toxicol. Pharmacol.*, 2015, **40**, 230–240.

41 K. Yao, P. P. Ye, L. Zhang, J. Tan, X. J. Tang and Y. D. Zhang, *Mol. Vision*, 2008, **14**, 217–223.

42 A. B. Karabulut, N. Karadag, S. Gurocak, T. Kiran, M. Tuzcu and K. Sahin, *Food Chem. Toxicol.*, 2014, **70**, 128–133.

43 T. Y. Forbes-Hernandez, F. Giampieri, M. Gasparini, L. Mazzoni, J. L. Quiles, J. M. Alvarez-Suarez and M. Battino, *Food Chem. Toxicol.*, 2014, **68**, 154–182.

44 I. Serraino, L. Dugo, P. Dugo, L. Mondello, E. Mazzon, G. Dugo, A. P. Caputi and S. Cuzzocrea, *Life Sci.*, 2003, **73**, 1097–1114.

45 D. Lu, A. Xu, H. Mai, J. Zhao, C. Zhang, R. Qi, H. Wang, D. Lu and L. Zhu, *Oxid. Med. Cell. Longevity*, 2015, **2015**, 437127.

46 C. Sina, A. Arlt, O. Gavrilova, E. Midtling, M. L. Kruse, S. S. Muerkoster, R. Kumar, U. R. Folsch, S. Schreiber, P. Rosenstiel and H. Schafer, *Inflammatory Bowel Dis.*, 2010, **16**, 320–331.

47 F. Christian, E. L. Smith and R. J. Carmody, *Cells*, 2016, **5**, 12.

48 S. K. S. Dev Kumar, V. Puri and S. Puri, *PLoS One*, 2015, **10**(1), e115947.

49 E.-W. L. Yu-Jin Hwang, J. Song, H.-R. Kim, Y.-C. Jun and K.-A. Hwang, *Sci. Rep.*, 2013, 1–10, DOI: 10.1038/srep03242.

50 A. Speciale, S. Anwar, R. Canali, J. Chirafisi, A. Saija, F. Virgili and F. Cimino, *Mol. Nutr. Food Res.*, 2013, **57**, 1979–1987.

51 Y. Y. Lee, J. S. Park, E. J. Lee, S. Y. Lee, D. H. Kim, J. L. Kang and H. S. Kim, *J. Agric. Food Chem.*, 2015, **63**, 3472–3480.

52 S. M. Kim, S. Y. Lee, J. S. Cho, S. M. Son, S. S. Choi, Y. P. Yun, H. S. Yoo, D. Y. Yoon, K. W. Oh, S. B. Han and J. T. Hong, *Eur. J. Pharmacol.*, 2010, **631**, 1–9.

53 G. H. Liu, J. Qu and X. Shen, *Biochim. Biophys. Acta*, 2008, **1783**, 713–727.

54 M. Yu, H. Li, Q. Liu, F. Liu, L. Tang, C. Li, Y. Yuan, Y. Zhan, W. Xu, W. Li, H. Chen, C. Ge, J. Wang and X. Yang, *Cell. Signalling*, 2011, **23**, 883–892.

